DOI: 10.1002/ejic.200801096

Selective Crystallization of Dimeric vs. Monomeric Dimethyltin-Containing Tungstoarsenates(III) and -antimonates(III) with the Guanidinium Cation

Santiago Reinoso,[a][‡] Michael H. Dickman,[a] and Ulrich Kortz*[a]

Keywords: Polyoxometalates / Tin / Organic–inorganic hybrid composites / Tungsten

The use of guanidinium cations $[C(NH_2)_3]^+$ as crystallizing agents allowed us to selectively isolate the dimeric $[\{(CH_3)_2Sn(H_2O)\}_4\{(CH_3)_2Sn\}(B\text{-}\beta\text{-}XW_9O_{33})_2]^{8-}$ (**1**, X = As^{III}; **2**, X = Sb^{III}) polyanions from the reaction of $(CH_3)_2SnCl_2$ with $Na_9[B\text{-}\alpha\text{-}XW_9O_{33}]$ (3:1 ratio) in water at pH 3. This reaction is known to give the monomeric $[\{(CH_3)_2Sn(H_2O)_2\}_3(B\text{-}\beta\text{-}XW_9O_{33})]^{3-}$ polyanions as the major species. Polyanions **1** and **2** are composed of one octahedral *trans*-$(CH_3)_2SnO_4$ moiety that bridges two trilacunary $[B\text{-}\beta\text{-}XW_9O_{33}]^{9-}$ Keggin subunits further decorated by two structurally nonequivalent $\{(CH_3)_2Sn\}^{2+}$ functionalities each: one distorted octahedral *trans*-$(CH_3)_2SnO_4$ linking moiety and one trigonal-bipyramidal *cis*-$(CH_3)_2SnO_3$ pendant group. This results in a dimeric, centrosymmetric assembly where each $[B\text{-}\beta\text{-}XW_9O_{33}]^{9-}$ subunit is connected to three $\{(CH_3)_2Sn\}^{2+}$ functionalities through two Sn–O(W) bonds. Polyanions **1** and **2** polymerize upon crystallization by forming intermolecular Sn–O–W bridges resulting in the isostructural hybrid materials $[C(NH_2)_3]_8[\{(CH_3)_2Sn(H_2O)\}_4\{(CH_3)_2Sn\}(B\text{-}\beta\text{-}XW_9O_{33})_2]\cdot 10H_2O$ (**1a**, X = As^{III}; **2a**, X = Sb^{III}). Compounds **1a** and **2a** were characterized in the solid state by elemental analysis, infrared spectroscopy, thermal analysis, and single-crystal X-ray diffraction. The crystal packing shows a 2D arrangement of the polyanions connected by the *trans*-$(CH_3)_2SnO_4$ linking moieties, resulting in corrugated hybrid layers parallel to the (101) plane with the *cis*-$(CH_3)_2SnO_3$ pendant groups acting as interlamellar spacers.

(© Wiley-VCH Verlag GmbH & Co. KGaA, 69451 Weinheim, Germany, 2009)

Introduction

Polyoxometalates (POMs) are anionic metal–oxygen clusters with a remarkable compositional, electronic, and structural diversity, and they have potential applications in a wide range of fields; the most active areas being catalysis and medicine because of the bifunctional acidic and redox properties as proton and electron reservoirs.[1] The mechanism of formation of POMs is commonly described as self-assembly and comprises a set of not well-understood equilibria affected by different factors, such as pH or temperature. Among these factors, the features of the countercation (type, size, shape) appear to be a key factor in the formation, stabilization, and final isolation of several POMs.[2] Therefore, the study of the countercation role remains an important research objective to allow for a rational design of tailored POM assemblies.

The properties of POMs can be enhanced or modified with the introduction of secondary functional groups, for example, through the covalent attachment of organic/organometallic moieties to the metal–oxo framework. Novel structural architectures and unexpected synergistic effects can be achieved from the combination of both components in a final hybrid species. Organotin groups are good candidates for the systematic derivatization of POMs because Sn^{IV} can substitute addenda metal centers in POM skeletons, and also because the Sn–C bond shows a relatively high stability to hydrolysis in aqueous media. In particular, mono-organotin moieties (RSn^{3+}) can be easily incorporated into the vacant sites of lacunary Keggin and Wells–Dawson heteropolytungstates, resulting in polysubstituted monomeric and dimeric polyanions containing tightly bound RSn^{3+} functionalities.[3] A few years ago, our group introduced the use of diorganotin units (R_2Sn^{2+}) as linkers of polytungstates and -molybdates to construct large, unprecedented assemblies (examples including monomeric to dodecameric discrete clusters),[4] or extended materials with dimensionalities ranging from 1 to 3.[5]

As a result of its planar geometry and high pK_a, the guanidinium cation $[C(NH_2)_3]^+$ undergoes strong hydrogen-bonding and charge-pairing interactions over a wide pH range with different anions, including POMs, in such a way that it can be employed to selectively crystallize species that are present in solution as minor species or cannot be isolated by using other types of standard cations (e.g., alkali ions).[2b,5b] Therefore, we decided to reinvestigate the reactivity of the $(CH_3)_2Sn^{2+}$ electrophile toward lacunary

[a] School of Engineering and Science, Jacobs University
P. O. Box 750 561, 28725 Bremen, Germany
E-mail: u.kortz@jacobs-university.de
[‡] Current address: Instituto de Ciencia Molecular (ICMol), Universidad de Valencia
Polígono de la Coma s/n, 46980 Paterna, Valencia, Spain

Supporting information for this article is available on the WWW under http://www.eurjic.org/ or from the author.

 © 2009 Wiley-VCH Verlag GmbH & Co. KGaA, Weinheim

Keggin and Wells–Dawson heteropolytungstates with $[C(NH_2)_3]^+$ as a countercation to study the effect of guanidinium as a selective crystallizing agent.

Here we report the synthesis, solid-state characterization, and crystal structure of the dimeric hybrid polyanions $[\{(CH_3)_2Sn(H_2O)\}_4\{(CH_3)_2Sn\}(B\text{-}\beta\text{-}XW_9O_{33})_2]^{8-}$ (**1**, X = As^{III}; **2**, X = Sb^{III}), which were isolated from the reaction of $(CH_3)_2SnCl_2$ with $Na_9[B\text{-}\alpha\text{-}XW_9O_{33}]$ (3:1 ratio) in water at pH 3, as the decahydrated guanidinium salts $[C(NH_2)_3]_8[\{(CH_3)_2Sn(H_2O)\}_4\{(CH_3)_2Sn\}(B\text{-}\beta\text{-}XW_9O_{33})_2]\cdot 10H_2O$ (**1a**, X = As^{III}; **2a**, X = Sb^{III}). In previous work,[4a] the same reaction conditions led to the monomeric polyanions $[\{(CH_3)_2Sn(H_2O)_2\}_3(B\text{-}\beta\text{-}XW_9O_{33})]^{3-}$ (**3**, X = As^{III}; **4**, X = Sb^{III}) isolated as the alkali salts $CsNa_2[\{(CH_3)_2Sn(H_2O)\}_2\{(CH_3)_2Sn(H_2O)_2\}(B\text{-}\beta\text{-}XW_9O_{33})_2]\cdot 7H_2O$ (**3a**, X = As^{III}; **4a**, X = Sb^{III}).

Results and Discussion

Synthesis

According to our previous work,[4a] heating an aqueous, acidic solution of $(CH_3)_2SnCl_2$ and $Na_9[B\text{-}\alpha\text{-}XW_9O_{33}]$ (X = As^{III}, Sb^{III}) in a 3:1 ratio at pH 3 for 1 h leads to the formation of monomeric, dimethyltin-containing $[\{(CH_3)_2Sn(H_2O)_2\}_3(B\text{-}\beta\text{-}XW_9O_{33})]^{3-}$ polyanions **3** (X = As^{III}) and **4** (X = Sb^{III}). These discrete polyanions are composed of a $[B\text{-}\beta\text{-}XW_9O_{33}]^{9-}$ trilacunary Keggin subunit stabilized by three $\{(CH_3)_2Sn\}^{2+}$ moieties grafted on the vacant positions through two Sn–O bonds each. As a result of the lability of the water molecules, polyanions **3** and **4** polymerize upon crystallization through the formation of intermolecular Sn–O_t–W bridges (O_t: terminal O atom). Thus, polyanions **3** and **4** were isolated in the solid state as the 2D alkaline salts $CsNa_2[\{(CH_3)_2Sn(H_2O)\}_2\{(CH_3)_2Sn(H_2O)_2\}(B\text{-}\beta\text{-}XW_9O_{33})_2]\cdot 7H_2O$ (**3a**, X = As^{III}; **4a**, X = Sb^{III}) following a direct crystallization strategy by addition of 1 M aqueous CsCl to the reaction mixture.

In order to investigate the effect of guanidinium cations as a selective crystallizing agent in the $(CH_3)_2Sn^{2+}/[B\text{-}\alpha\text{-}XW_9O_{33}]^{9-}$ (X = As^{III}, Sb^{III}) system, we decided to perform the reaction under the same conditions, but by using 1 M aqueous $[C(NH_2)_3]Cl$ instead of CsCl for the direct crystallization step. As a result, we were able to isolate the guanidinium salts $[C(NH_2)_3]_8[\{(CH_3)_2Sn(H_2O)\}_4\{(CH_3)_2Sn\}(B\text{-}\beta\text{-}XW_9O_{33})_2]\cdot 10H_2O$ (**1a**, X = As^{III}; **2a**, X = Sb^{III}) from the reaction mixture. Compounds **1a** and **2a** are also 2D assemblies formed by polymerization of dimethyltin-containing polyanions through the formation of Sn–O_t–W bridges, but unlike the alkali cations, the structures of these salts are based on the dimeric species $[\{(CH_3)_2Sn(H_2O)_2\}_4\{(CH_3)_2Sn\}(B\text{-}\beta\text{-}XW_9O_{33})_2]^{8-}$ (**1**, X = As^{III}; **2**, X = Sb^{III}) instead of monomeric building blocks **3** and **4**. Polyanions **1** and **2** are composed of one bridging $\{(CH_3)_2Sn\}^{2+}$ moiety that links two $[B\text{-}\beta\text{-}XW_9O_{33}]^{9-}$ subunits further decorated by two $\{(CH_3)_2Sn\}^{2+}$ groups each, in such a way that each trilacunary Keggin cluster is linked to three dimethyltin functionalities with a connectivity pattern similar to that observed for related monomeric polyanions **3** and **4**. Compounds **1a** and **2a** were also obtained in moderate to good yields when the reaction was carried out at room temperature, at pH values up to 6, or with a $(CH_3)_2Sn^{2+}/[B\text{-}\alpha\text{-}XW_9O_{33}]^{9-}$ ratio of 2:1, but they were not formed when the pH of the reaction mixture was adjusted to 2 or lower values.

Formation of polyanions **1**–**4** involves isomerization of the trilacunary Keggin precursor from the *B*-*α* to the *B*-*β* form by a 60° rotation of a W_3O_{13} triad upon reaction with the $(CH_3)_2Sn^{2+}$ electrophile. Although this isomerization is known to be facilitated in aqueous, acidic solutions such as our reaction media,[6] we believe that in our case the main driving force for the *B*-*α* to *B*-*β* transformation is the grafting of the $(CH_3)_2Sn^{2+}$ moieties onto the POM framework on the basis of the fact that polyanions **1** and **2** are also obtained in moderate to good yields under only slightly acidic synthetic conditions (pH 6). The internal methyl groups of the hypothetical trisubstituted α-derivatives of polyanions **1**–**4** would be too close to each other and to the lone pair of electrons of the heteroatom, leading to repulsive steric and electronic interactions, which destabilize these assemblies based on *α*-derivatives.

At around pH 3, the predominant species in solution formed from the reaction of the $(CH_3)_2Sn^{2+}$ electrophile with the lacunary $[B\text{-}\alpha\text{-}XW_9O_{33}]^{9-}$ (X = As^{III}, Sb^{III}) heteropolytungstates are monomeric $[\{(CH_3)_2Sn(H_2O)_2\}_3(B\text{-}\beta\text{-}XW_9O_{33})]^{3-}$ polyanions **3** and **4**, as indicated by the comparison of the multinuclear (^{183}W, ^{119}Sn, ^{13}C, ^1H) NMR spectra performed on freshly prepared reaction mixtures or on solid samples of compounds **3a** and **4a** redissolved in water. These NMR spectra remain unchanged for several months, indicating that monomeric species **3** and **4** are stable in solution and do not undergo any further structural transformation to dimeric polyanions **1** and **2**, respectively.[4a] We discovered that the ^{183}W NMR spectrum of the reaction mixture containing the Sb^{III}–POM precursor showed an additional, very small peak that probably corresponds to another, unidentified species present in solution. Considering these observations, dimeric polyanions **1** and **2** are most likely formed as side products in addition to monomeric main products **3** and **4** when the $(CH_3)_2Sn^{2+}$ electrophile reacts with the lacunary $[B\text{-}\alpha\text{-}XW_9O_{33}]^{9-}$ precursors. Therefore, we believe that polyanions **1** and **2** do actually exist in solution in low concentration as minor species and that they are in equilibrium with predominant monomeric species **3** and **4**, respectively. In this way, whereas **3** and **4** are obtained in the solid state as compounds **3a** and **4a** with alkali cations, the use of the guanidinium ion as a crystallizing agent allowed us to selectively isolate **1** and **2** in fairly good yields from the reaction mixture as compounds **1a** and **2a**, respectively.

Infrared Spectroscopy and Thermal Analysis

The infrared spectra of compounds **1a** and **2a** unambiguously indicate the presence of the $(CH_3)_2Sn^{2+}$ moiety in

 © 2009 Wiley-VCH Verlag GmbH & Co. KGaA, Weinheim

both compounds (Figure S1, Supporting Information). These spectra display single peaks of weak intensity around 1200 cm^{-1} (**1a**, 1192; **2a**, 1194 cm^{-1}), which are characteristic of methyltin(IV) derivatives and can be assigned to the symmetrical bending vibration mode of the methyl groups [$\delta_s(CH_3)$].[7]

The bands in the region below 1000 cm^{-1} are attributed to the stretching and bending modes of the metal–oxo polyanion bonds. Polyanions **1** and **2** show similar spectra with two strong peaks at approximately 940 and 865 cm^{-1}, which can be attributed to the antisymmetric stretching vibrations of the X–O and W–O_t bonds [ν_{as}(W–O_t) and ν_{as}(W–O_t) + ν_{as}(X–O), respectively], four strong to very strong bands in the range 810–670 cm^{-1}, which originate from the antisymmetric stretching of the (Sn)W–O–W(Sn) bridges [ν_{as}(M–O_b–M), where O_b: bridging oxygen atom], and at least three medium intensity peaks below 520 cm^{-1}, which correspond to bending vibrations of the central XO_4 group and the (Sn)W–O–W(Sn) bridges [δ(O–X–O) + δ(M–O_b–M)]. The bands associated with the (Sn)W–O–W(Sn) bridges in compound **1a** are, in general, approximately 10 cm^{-1} blueshifted with respect to those of **2a**. This phenomenon indicates shorter bridging metal–oxygen bonds and a subsequent contraction of the $\{W_9O_{33}\}$ POM skeleton of polyanion **1**, reflecting the smaller size of the As^{III} heteroatom with respect to Sb^{III}.

Comparing the infrared spectra of polyanions **1** and **2** with those of **3** and **4** reveals an almost identical overall shape below 1000 cm^{-1} with significant changes in only a few band positions. This is in complete agreement with the fact that, besides being composed of the same building blocks, in all four species each [*B*-β-XW_9O_{33}]$^{9-}$ subunit is linked to three dimethyltin moieties with a similar connectivity pattern. The main differences are encountered in the bands originating from the ν_{as}(W–O_t) vibration mode and some of the bands associated to the ν_{as}(M–O_b–M) vibration mode, which are approximately 10 cm^{-1} redshifted in **1** and **2** with respect to the infrared spectra of **3** and **4**, respectively. This effect can be attributed to the massive network of strong N–H···O hydrogen bonds between the guanidinium cations and the O_t and O_b atoms present in the crystal packing of compounds **1a** and **2a**.[8]

Thermal analysis under a nitrogen atmosphere shows that compounds **1a** and **2a** decompose by three consecutive mass loss steps (Figure S2, Supporting Information). Decomposition starts at room temperature with an endothermic dehydration step around 185 and 190 °C for compounds **1a** and **2a**, respectively. This step involves the loss of the water molecules of both hydration and coordination [% calcd. (found) for $14H_2O$: **1a**, 4.21 (4.23); **2a**, 4.14 (4.01)]. The second step for **1a** comprises two different, highly overlapping processes: the endothermic release of the guanidinium cations in the range from 185 to approximately 355 °C, followed by the exothermic loss of the methyl groups up to 455 °C [% calcd. (found) for $C_8N_{24}H_{48}$ + $C_{10}H_{30}$: 10.53 (11.08)]. Immediately after loss of the organic component, **1a** undergoes decomposition of the resulting metal–oxo framework in an exothermic third step, leading to a thermally stable residue above 685 °C [% calcd. (found) for $As_2Sn_5W_{18}O_{54}$: 82.06 (82.35)]. In contrast to **1a**, the second step in the case of **2a** can be exclusively attributed to the endothermic release of the guanidinium cations below 370 °C [% calcd. (found) for $C_8N_{24}H_{48}$: 7.90 (8.39)]. The third step involves at least two highly overlapping exothermic processes, which can be assigned to the loss of the methyl groups around approximately 435 °C [% calcd. (found) for $C_{10}H_{30}$: 2.47 (1.74)], followed by decomposition of the resulting metal–oxo framework. As for **1a**, a thermally stable residue is obtained above 685 °C [% calcd. (found) for $Sb_2Sn_5W_{18}O_{67}$: 85.75 (86.06)].

Structure of Polyanions 1 and 2

Polyanions **1** and **2** consist of two [*B*-β-XW_9O_{33}]$^{9-}$ subunits (X = As^{III} and Sb^{III}, respectively) linked by one bridging $\{(CH_3)_2Sn\}^{2+}$ moiety. The [*B*-β-XW_9O_{33}]$^{9-}$ subunits are further decorated by two structurally nonequivalent $\{(CH_3)_2Sn\}^{2+}$ groups each, leading to a dimeric, centrosymmetric assembly. Each trilacunary Keggin fragment is connected to three dimethyltin functionalities, and the bridging moiety lies on the center of inversion (Figure 1).

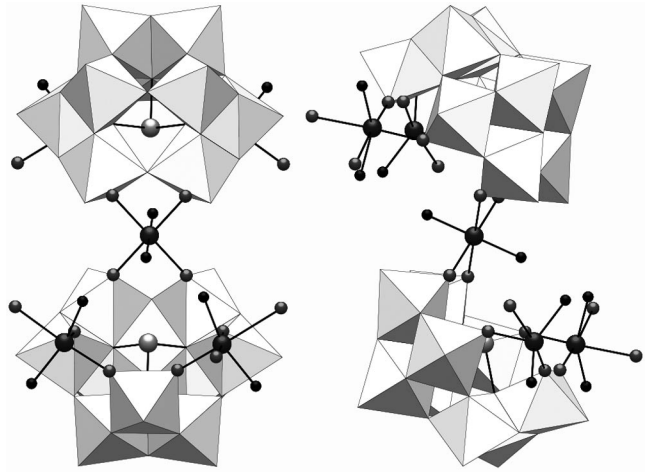

Figure 1. Front (left) and side (right) polyhedral/ball-and-stick representations of polyanions **1** and **2**. Color code: WO_6 octahedra, white; Sn, dark grey; C, black; O, grey; X = As (**1**), Sb (**2**), light grey.

The parent [α-$XW_{12}O_{40}$]$^{4-}$ Keggin anion consists of a central XO_4 tetrahedral hetero group and four W_3O_{13} triads (composed of three edge-sharing WO_6 octahedra) linked through corner-sharing resulting in a polyanion with ideal T_d symmetry. The [*B*-β-$X^{III}W_9O_{33}$]$^{9-}$ trilacunary species can be derived from the parent cluster by removal of one W_3O_{13} triad, followed by a 60° rotation of another W_3O_{13} triad and replacement of the terminal O atom of the XO_4 heterogroup by a lone pair of electrons. Besides compounds **3a** and **4a**,[4a] the (*B*-β-XW_9O_{33}) (X = As^{III} Sb^{III}) fragments were observed in several Krebs-type derivatives $\{M_4X_2W_{18}O_{76}\}$,[6,9] in the large tungstoarsenate(III) $[As_6W_{65}O_{217}(H_2O)_7]^{26-}$,[10] and in the tungstoantimon-

 © 2009 Wiley-VCH Verlag GmbH & Co. KGaA, Weinheim

ate(III) $[Na_2Sb_8W_{36}O_{132}(H_2O)_4]^{22-}$.[6a] To the best of our knowledge no structural characterization of the [*B*-*β*-$XW_9O_{33}]^{9-}$ (X = As^{III} Sb^{III}) clusters alone can be found in the literature. The W–O bond lengths in the [*B*-*β*-$XW_9O_{33}]^{9-}$ subunits of **1** and **2** fall within normal ranges, and the W–O(Sn) bonds [**1**, 1.789(10)–1.841(9); **2**, 1.801(12)–1.863(11) Å] are significantly shorter than the W–O(W) bonds [**1**, 1.862(9)–2.049(9); **2**, 1.816(12)–2.071(12) Å] as previously observed for other organotin-containing heteropolytungstates.[3a] In addition, the Keggin frameworks in **1** and **2** display a general distortion consisting of sequences of *trans*-related short and long bond alternations that propagate through the POM skeleton starting either from the W–O(Sn) bonds or from the rotated W_3O_{13} triad and ending at the opposite W5–W8 or W6–W7 pairs of atoms, respectively (Figure 2).[3k]

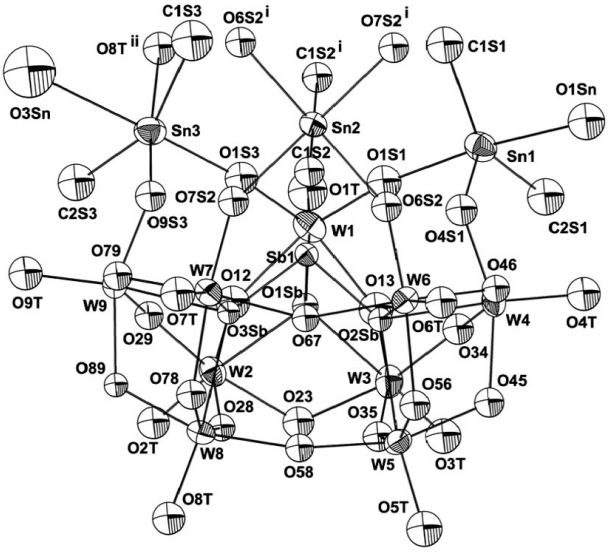

Figure 2. ORTEP view and labeling scheme of the asymmetric unit of [{$(CH_3)_2Sn(H_2O)$}$_4${$(CH_3)_2Sn$}(*B*-*β*-$SbW_9O_{33})_2]^{8-}$ (**2**) in compound **2a**; 50% probability displacement ellipsoids; hydrogen atoms have been omitted for clarity. This figure is also representative for the As analogue [{$(CH_3)_2Sn(H_2O)$}$_4${$(CH_3)_2Sn$}(*B*-*β*-$AsW_9O_{33})_2]^{8-}$ (**1**) in compound **1a**. Symmetry codes: i) –*x*, –*y* + 1, – *z*; ii) –*x* – 1/2, *y* + 1/2, –*z* + 1/2.

Polyanions **1** and **2** contain five $\{(CH_3)_2Sn\}^{2+}$ functionalities, which can be classified into three different types based on their structural role: one functionality (Sn2) acts as a bridging moiety between the two trilacunary subunits of the same polyanion, another two (Sn3/Sn3^i) link neighboring polyanions into extended assemblies, and the remaining two functionalities (Sn1/Sn1^i) are pendant groups (Figure 2). The $\{(CH_3)_2Sn\}^{2+}$ functionalities are grafted onto the vacant positions of the trilacunary subunits through two Sn–O bonds each, in such a way that the bridging moiety Sn2 is attached to two pairs of corner-shared WO_6 octahedra from the nonrotated W_3O_{13} triads, whereas the Sn3/Sn1 and Sn3^i/Sn1^i groups are connected by the rotated W_3O_{13} triad through the $W1O_6$ octahedron.

Selected bond lengths and angles for the Sn centers in polyanions **1** and **2** are summarized in Table 1. The Sn2 atom in the bridging moiety lies on a center of inversion, displaying a regular octahedral *trans*-$(CH_3)_2SnO_4$ coordination geometry. The O6S2/O7S2 and O6S2^i/O7S2^i pairs of terminal O atoms form the equatorial plane with medium Sn–O bond lengths of approximately 2.20 Å and the methyl groups occupy the axial positions in a *trans* arrangement with usual Sn–C bond lengths of around 2.10 Å. The coordination environment around the Sn3 atoms in the linking moieties is also octahedral *trans*-$(CH_3)_2SnO_4$, with the axial positions occupied by the methyl groups in a relative *trans* arrangement, and the equatorial plane defined by the terminal O1S3 and O9S3 atoms of the trilacunary Keggin subunits, one water molecule of coordination (O3Sn), and the terminal O8T^{ii} atom belonging to a neighboring polyanion. However, the octahedral geometry of the Sn3 atom is highly distorted in comparison to that of the Sn2 center: the C–Sn–C deviates significantly from linearity (~150°) and the equatorial bonding can be described as two short (Sn3–O1S3 and Sn3–O9S3), one long (Sn3–O8T^{ii}), and one very long (Sn3–O3Sn) bonds. These geometric parameters are in agreement with those observed for other polytungstates containing octahedral *trans*-$(CH_3)_2SnO_4$ moieties.[4] In contrast to Sn2 and Sn3, the Sn1 centers in the pendant groups are pentacoordinate and exhibit a highly distorted *cis*-$(CH_3)_2SnO_3$ coordination sphere that is best described as trigonal-bipyramidal. The equatorial plane is composed of the terminal O4S1 atom and the two methyl groups, which therefore display a relative *cis* arrangement. The coordination sphere is completed by the terminal O1S1 atom and one water molecule of coordination (O1Sn) in the axial positions. All the Sn–C and Sn–O bonds are short, with the

Table 1. Selected bond lengths [Å] and angles [°] for the tin atoms in polyanions **1** and **2**.[a]

	1	**2**
Sn1–C1S1	2.084(15)	2.100(19)
Sn1–C2S1	2.092(15)	2.071(19)
Sn1–O1S1	2.102(10)	2.102(12)
Sn1–O1Sn	2.454(11)	2.450(13)
Sn1–O4S1	2.037(9)	2.019(11)
C1S1–Sn1–C2S1	139.3(6)	140.6(8)
Sn2–C1S2	2.121(13)	2.096(15)
Sn2–C1S2^i	2.121(13)	2.096(15)
Sn2–O6S2	2.184(9)	2.212(10)
Sn2–O6S2^i	2.184(9)	2.212(10)
Sn2–O7S2	2.193(9)	2.223(10)
Sn2–O7S2^i	2.193(9)	2.233(10)
C1S2–Sn2–C1S2^i	180	180
Sn3–C1S3	2.102(16)	2.10(2)
Sn3–C2S3	2.095(17)	2.120(19)
Sn3–O1S3	2.033(10)	2.045(11)
Sn3–O3Sn	2.790(19)	2.74(2)
Sn3–O8T^{ii}	2.538(9)	2.533(11)
Sn3–O9S3	2.100(9)	2.100(11)
C1S3–Sn3–C2S3	150.2(7)	152.3(8)

[a] Symmetry codes: i) –*x*, –*y* + 1, –*z*; ii) –*x* – 1/2, *y* + 1/2, –*z* + 1/2.

 © 2009 Wiley-VCH Verlag GmbH & Co. KGaA, Weinheim

exception of the long Sn–O1Sn bond, whereas the distortion of the ideal trigonal-bipyramidal geometry is well reflected by both the equatorial C–Sn–C and the axial O–Sn–O [**1**, 166.3(4); **2**, 168.0(4)°] bond angles, also common for the *cis*-$(CH_3)_2SnO_3$ groups of some of our previously reported dimethyltin-containing polyanions.[4h,5] The assignment of the O1Sn and O3Sn atoms as water molecules is supported by bond valence sum (BVS) calculations,[11] which clearly indicate that these two oxo ligands are diprotonated in agreement with the results of the elemental and thermal analyses.

Crystal Packing of Compounds 1a and 2a

The crystal packing of the isostructural compounds **1a** and **2a** shows that polyanions **1** or **2** are connected by the *trans*-$(CH_3)_2SnO_4$ linking moieties, resulting in a 2D hybrid organic–inorganic POM assembly (Figure 3). Each polyanion is connected to the four nearest neighbors by four linking moieties and, more specifically, through equatorial coordination of the Sn3 centers to the terminal O1S3 and O9S3 atoms of one polyanion and to the terminal O8T atom of a neighboring polyanion. In agreement with the solution properties of the related 2D materials **3a** and **4a**,[4a] polymeric **1a** and **2a** most likely start to decompose in solution by rupture of the long Sn3–O8T^{ii} bonds resulting in discrete molecular **1** and **2**, respectively. The sixth position in the coordination sphere of Sn3 is then almost certainly occupied by a labile water molecule, although changes in the coordination number/geometry of Sn3 to trigonal-bipyramidal or of Sn1 to distorted octahedral cannot be disregarded due to the flexible coordination properties of the Sn centers. In the first case, the C_i symmetry observed by X-ray diffraction would be maintained, whereas in the other two cases polyanions **1** and **2** would display C_{2h} point-group symmetry. We tried to perform solution ^{183}W and ^{119}Sn NMR experiments to ascertain this point, but the low solubility of **1a** and **2a** did not allow us to obtain useful results.

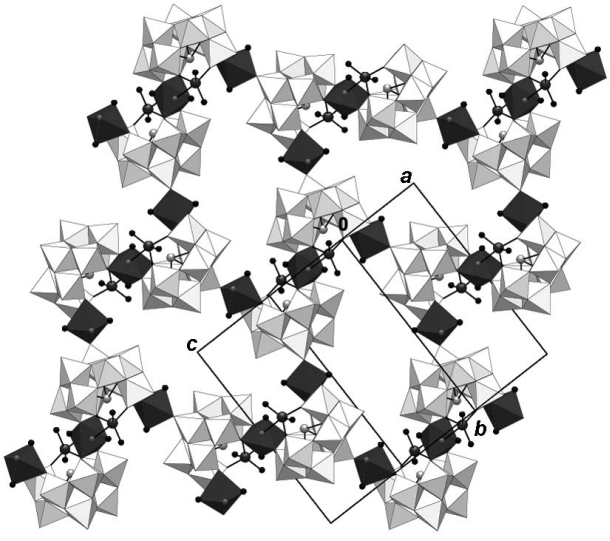

Figure 3. Polyhedral/ball-and-stick projection of the (201) plane of the 2D arrangement of polyanions **1** and **2** in the crystal packing of compounds **1a** and **2a**, respectively. Color code: same as Figure 1; the inner coordination spheres of Sn2 and Sn3 are shown as polyhedra in order to highlight the backbone of the hybrid layer.

Polyanions **1** and **2** are arranged in corrugated hybrid layers where the bridging and linking dimethyltin moieties (Sn2 and Sn3 centers) are located in planes parallel to the (101) plane. These layers pack along the crystallographic *a* axis with the pendant dimethyltin groups (Sn1 centers) pointing to the interlamellar space. Thus, the pendant groups act as interlamellar spacers, leading to an open-framework crystal packing with elliptical channels parallel to the [010] direction (Figure 4). These channels host both the guanidinium cations and the water molecules of hydration, in such a way that an extended and intricate network of strong N–H···O_{POM} and O–H···O_{POM} hydrogen bonds holds the hybrid layers together.

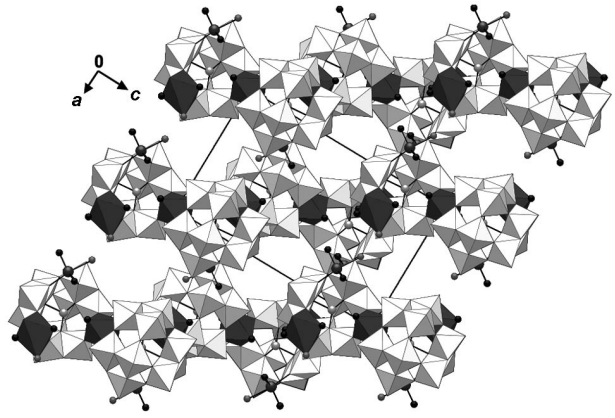

Figure 4. View of the crystal packing of compounds **1a** and **2a** along the [010] direction. Guanidinium cations and hydration water molecules, which are located in the channels parallel to the crystallographic *b* axis, are not shown for clarity. Color code: same as Figure 1.

Conclusions

This work constitutes a nice example of how the guanidinium cation $[C(NH_2)_3]^+$ can be employed as an effective crystallizing agent for the selective solid-state isolation of organotin-containing hybrid polyanions that are present in solution as minor species and cannot be isolated by using other types of standard cations (e.g., alkali ions). In our particular case, we have shown that the use of guanidinium cations allowed us to selectively isolate dimeric $[\{(CH_3)_2Sn(H_2O)\}_4\{(CH_3)_2Sn\}(B\text{-}\beta\text{-}XW_9O_{33})_2]^{8-}$ (**1**, X = As^{III}; **2**, X = Sb^{III}) polyanions from the reaction of $(CH_3)_2SnCl_2$ with $Na_9[B\text{-}\alpha\text{-}XW_9O_{33}]$ (3:1 ratio) in water at pH 3. It must be remembered that the major species formed in this reaction are the monomeric $[\{(CH_3)_2Sn(H_2O)_2\}_3(B\text{-}\beta\text{-}XW_9O_{33})]^{3-}$ polyanions, as indicated by multinuclear NMR solution studies, and that the addition of alkali cations to the reaction mixture leads to the formation of 2D hybrid materials based on these monomeric building blocks.[3a] Polyanions **1** and **2** are composed of one octahedral *trans*-$(CH_3)_2SnO_4$ moiety bridging two trilacunary $[B\text{-}\beta\text{-}XW_9O_{33}]^{9-}$ Keggin

 © 2009 Wiley-VCH Verlag GmbH & Co. KGaA, Weinheim

subunits, which are further decorated by two structurally nonequivalent $\{(CH_3)_2Sn\}^{2+}$ functionalities each: one distorted octahedral *trans*-$(CH_3)_2SnO_4$ linking moiety and one trigonal-bipyramidal *cis*-$(CH_3)_2SnO_3$ pendant group. This results in a dimeric, centrosymmetric assembly where each $[B\text{-}\beta\text{-}XW_9O_{33}]^{9-}$ subunit is connected to three $\{(CH_3)_2Sn\}^{2+}$ functionalities through two Sn–O(W) bonds. Polyanions **1** and **2** polymerize upon crystallization through the formation of intermolecular Sn–O–W bridges, which leads to the isostructural salts $[C(NH_2)_3]_8[\{(CH_3)_2Sn(H_2O)\}_4\{(CH_3)_2Sn\}(B\text{-}\beta\text{-}XW_9O_{33})_2]\cdot 10H_2O$ (**1a**, X = As^{III}; **2a**, X = Sb^{III}). The crystal packing of compounds **1a** and **2a** shows a 2D arrangement of Keggin polyanion fragments connected by the *trans*-$(CH_3)_2SnO_4$ linking moieties, resulting in corrugated hybrid layers parallel to the (101) plane with the *cis*-$(CH_3)_2SnO_3$ pendant groups acting as interlamellar spacers. Currently, we extend this investigation to the reactivity of the $(CH_3)_2Sn^{3+}$ electrophile toward other lacunary Keggin and Wells–Dawson-type heteropolytungstates.

Experimental Section

General Remarks: The POM precursor salts $Na_9[B\text{-}\alpha\text{-}XW_9O_{33}]\cdot\sim 20H_2O$ (X = As^{III}, Sb^{III}) were synthesized according to literature procedures and identified by infrared spectroscopy.[6a,12] All other chemicals were purchased from commercial sources and used without further purification. Elemental analyses were performed on dehydrated samples by Eurofins Umwelt West GmbH, Wesseling, Germany. Infrared spectra for solid samples were obtained as KBr pellets with a Nicolet Avatar 370 FTIR spectrophotometer. Thermal analyses were carried out with a TA Instruments SDT Q600 thermobalance with a 100 mL min^{-1} flow of nitrogen; the temperature was ramped from 20 to 800 °C at a rate of 5 °C min^{-1}.

$[C(NH_2)_3]_8[\{(CH_3)_2Sn(H_2O)\}_4\{(CH_3)_2Sn\}(B\text{-}\beta\text{-}AsW_9O_{33})_2]\cdot 10H_2O$ (1a): Powdered $Na_9[B\text{-}\alpha\text{-}AsW_9O_{33}]\cdot\sim 20H_2O$ (0.56 g, 0.20 mmol) was added to a solution of $(CH_3)_2SnCl_2$ (0.13 g, 0.60 mmol) in water (30 mL), and the pH of the resulting solution was adjusted to 3.0 with aqueous 1 M HCl. After heating at 80 °C for 1 h, the solution was cooled to room temperature and then a few drops of aqueous 1 M $[C(NH_2)_3]Cl$ was added. Colorless, block-shaped single crystals of **1a** suitable for X-ray diffraction were obtained by slow evaporation at room temperature for a few days. Yield: 0.23 g (39% based on As). $C_{18}H_{78}As_2N_{24}O_{66}Sn_5W_{18}$ (5739.4): calcd. C 3.77, H 1.37, As 2.6, N 5.86, Sn 10.3, W 57.7; found C 3.74, H 1.25, As 2.5, N 5.73, Sn 11.5, W 57.6. IR: $\tilde{\nu}$ = 1192 (w), 1119 (sh.), 944 (s), 869 (s), 812 (vs), 760 (vs), 722 (s), 677 (s), 571 (sh.), 518 (m), 474 (m), 417 (m) cm^{-1}.

$[C(NH_2)_3]_8[\{(CH_3)_2Sn(H_2O)\}_4\{(CH_3)_2Sn\}(B\text{-}\beta\text{-}SbW_9O_{33})_2]\cdot 10H_2O$ (2a): Compound **2a** was prepared following the same procedure as described above for **1a**, but by using $Na_9[B\text{-}\alpha\text{-}SbW_9O_{33}]\cdot\sim 20H_2O$ (0.57 g, 0.20 mmol) as the POM precursor. Colorless, block-shaped single crystals of **2a** suitable for X-ray diffraction were obtained by slow evaporation at room temperature for a few days. Yield: 0.27 g (45% based on Sb). $C_{18}H_{78}N_{24}O_{66}Sb_2Sn_5W_{18}$ (5833.1): calcd. C 3.71, H 1.35, N 5.76, Sb 4.2, Sn 10.2, W 56.7; found C 3.63, H 1.03, N 5.66, Sb 4.4, Sn 10.8, W 58.8. IR: $\tilde{\nu}$ = 1194 (w), 1116 (sh.), 941 (s), 863 (s), 797 (sh.), 750 (vs), 698 (sh.), 667 (s), 563 (sh.), 520 (m), 460 (m), 422 (m), 451 (s), 420 (m) cm^{-1}.

X-ray Crystallography: Crystallographic data for compounds **1a** and **2a** are summarized in Table 2. Single crystals were mounted in Hampton cryoloops (**1a**) or on glass fibers (**2a**) for indexing and intensity data collection at 173 or 296 K, respectively. Data were collected with a Bruker X8 APEX II CCD single-crystal diffractometer with κ geometry and graphite-monochromated Mo-K_α radiation (λ = 0.71073 Å). Data collection, unit cell determinations, intensity data integrations, routine corrections for Lorentz and polarization effects, and multiscan absorption corrections were performed by using the APEX2 software package.[13] The structures were solved and refined by using the SHELXTL software package.[14] Direct methods were used to solve the structures and to locate the heavy atoms. The remaining atoms were found from successive Fourier syntheses. Heavy atoms were refined anisotropically. Hydrogen atoms of the methyl groups and the guanidinium cations were placed in calculated positions and were refined with a riding model by using standard SHELXL parameters. For **1a** the guanidinium cations were restrained to be planar with similar C–N distances (FLAT and SADI restraints). Additionally, one W_3O_{13} edge-shared triad composed of W1, W2, and W3 was apparently disordered, containing about 5% of the corresponding α isomer (triad back-rotated by 60°). The 5% disordered W atoms were included with freely refined isotropic thermal parameters but no oxygen atoms associated with the disordered W atoms were modeled. For both compounds, final geometrical calculations were carried out with the PLATON program.[15] CCDC-704756 (for **1a**) and -704757 (for **2a**) contain the supplementary crystallographic data for this paper. These data can be obtained free of charge from The Cambridge Crystallographic Data Centre via www.ccdc.cam.ac.uk/data_request/cif.

Table 2. Crystallographic data for compounds **1a** and **2a**.[a]

	1a	**2a**
Formula	$C_{18}H_{106}N_{24}As_2O_{80}Sn_5W_{18}$	$C_{18}H_{106}N_{24}O_{80}Sb_2Sn_5W_{18}$
Fw [g mol^{-1}]	5991.9	6085.2
Crystal system	monoclinic	monoclinic
Space group	$P2_1/n$	$P2_1/n$
T [K]	173(2)	296(2)
a [Å]	12.9690(16)	12.9497(3)
b [Å]	19.469(2)	19.3214(4)
c [Å]	20.593(3)	20.9501(4)
β [°]	90.169(8)	90.2052(11)
V [Å^3]	5199.6(12)	5241.81(19)
Z	2	2
$\rho_{calcd.}$ [g cm^{-3}]	3.827	3.856
μ [mm^{-1}]	21.738	21.440
Reflections		
Collected	242219	251707
Unique (R_{int})	13333 (0.112)	12034 (0.102)
Observed	9941 ($I > 2\sigma I$)	9502 ($I > 2\sigma I$)
Parameters	367	343
$R(F)$ ($I > 2\sigma I$)	0.046	0.048
$wR(F^2)$ (all data)	0.121	0.130
GoF	1.04	1.05

[a] $R(F) = \Sigma\ ||F_o| - |F_c||/\Sigma\ |F_o|$; $wR(F^2) = \{\Sigma\ [w(F_o^2 - F_c^2)^2]/\Sigma\ [w(F_o^2)^2]\}^{1/2}$.

Supporting Information (see footnote on the first page of this article): Fourier transform infrared spectra and thermogravimetric curves for compounds **1a** and **2a**.

Acknowledgments

U. K. thanks Jacobs University and the Fonds der Chemischen Industrie for research support. S. R. thanks Gobierno Vasco/Eusko Jaurlaritza for his postdoctoral fellowship.

 © 2009 Wiley-VCH Verlag GmbH & Co. KGaA, Weinheim

[1] a) M. T. Pope, *Heteropoly and Isopoly Oxometalates*, Springer, Berlin, Germany, **1983**; b) M. T. Pope, A. Müller, *Angew. Chem. Int. Ed. Engl.* **1991**, *30*, 34–48; c) M. T. Pope, A. Müller (Eds.), *Polyoxometalates: From Platonic Solids to Antiretroviral Activity*, Kluwer, Dordrecht, The Netherlands, **1994**; d) *Chem. Rev.* **1998**, 98(1), special thematic issue; e) M. T. Pope, A. Müller (Eds.), *Polyoxometalate Chemistry: From Topology via self-Assembly to Applications*, Kluwer, Dordrecht, The Netherlands, **2001**; f) M. T. Pope, T. Yamase (Eds.), *Polyoxometalate Chemistry for Nanocomposite Design*, Kluwer, Dordrecht, The Netherlands, **2002**; g) J. J. Borrás-Almenar, E. Coronado, A. Müller, M. T. Pope (Eds.), *Polyoxometalate Molecular Science*, Kluwer, Dordrecht, The Netherlands, **2003**; h) M. T. Pope in *Comprehensive Coordination Chemistry II* (Eds: J. A. McCleverty, T. J. Meyer), Elsevier, Oxford, UK, **2004**.

[2] See for example: a) D.-L. Long, P. Kögerler, L. J. Farrugia, L. Cronin, *Angew. Chem. Int. Ed.* **2003**, *42*, 4180–4183; b) C. Streb, D.-L. Long, L. Cronin, *CrystEngComm* **2006**, *8*, 629–634; c) D.-L. Long, E. Burkholder, L. Cronin, *Chem. Soc. Rev.* **2007**, *36*, 105–121.

[3] For some examples, see: a) F. Xin, M. T. Pope, *Organometallics* **1994**, *13*, 4881–4886; b) F. Xin, M. T. Pope, G. J. Long, U. Russo, *Inorg. Chem.* **1996**, *35*, 1207–1213; c) F. Xin, M. T. Pope, *Inorg. Chem.* **1996**, *35*, 5693–5695; d) G. Sazani, M. H. Dickman, M. T. Pope, *Inorg. Chem.* **2000**, *39*, 939–943; e) S. Bareyt, S. Piligkos, B. Hasenknopf, P. Gouzerh, E. Lacôte, S. Thorimbert, M. Malacria, *Angew. Chem. Int. Ed.* **2003**, *42*, 3404–3406; f) G. Sazani, M. T. Pope, *Dalton Trans.* **2004**, 1989–1994; g) F. Hussain, U. Kortz, R. J. Clark, *Inorg. Chem.* **2004**, *43*, 3237–3241; h) S. Bareyt, S. Piligkos, B. Hasenknopf, P. Gouzerh, E. Lacôte, S. Thorimbert, M. Malacria, *J. Am. Chem. Soc.* **2005**, *127*, 6788–6794; i) N. Belai, M. T. Pope, *Polyhedron* **2006**, *25*, 2015–2020; j) K. Micoine, B. Hasenknopf, S. Thorimbert, E. Lacôte, M. Malacria, *Org. Lett.* **2007**, *9*, 3981–3984; k) S. Reinoso, M. H. Dickman, A. Praetorius, L. F. Piedra-Garza, U. Kortz, *Inorg. Chem.* **2008**, *47*, 8798–8806.

[4] a) F. Hussain, M. Reicke, U. Kortz, *Eur. J. Inorg. Chem.* **2004**, 2733–2738; b) F. Hussain, U. Kortz, *Chem. Commun.* **2005**, 1191–1193; c) U. Kortz, F. Hussain, M. Reicke, *Angew. Chem. Int. Ed.* **2005**, *44*, 3773–3777; d) F. Hussain, U. Kortz, B. Keita, L. Nadjo, M. T. Pope, *Inorg. Chem.* **2006**, *45*, 761–766; e) M. S. Alam, V. Dremov, P. Müller, A. V. Postnikov, S. S. Mal, F. Hussain, U. Kortz, *Inorg. Chem.* **2006**, *45*, 2866–2872; f) F. Hussain, M. H. Dickman, U. Kortz, B. Keita, L. Nadjo, G. A. Khitrov, A. G. Marshall, *J. Cluster Sci.* **2007**, *18*, 173–191; g) B. Keita, P. de Oliveira, L. Nadjo, U. Kortz, *Chem. Eur. J.* **2007**, *13*, 5480–5491; h) S. Reinoso, M. H. Dickman, M. F. Matei, U. Kortz, *Inorg. Chem.* **2007**, *46*, 4383–4385.

[5] a) S. Reinoso, M. H. Dickman, M. Reicke, U. Kortz, *Inorg. Chem.* **2006**, *45*, 9014–9019; b) S. Reinoso, M. H. Dickman, U. Kortz, *Inorg. Chem.* **2006**, *45*, 10422–10424.

[6] a) M. Bösing, I. Loose, H. Pohlmann, B. Krebs, *Chem. Eur. J.* **1997**, *3*, 1232–1237; b) U. Kortz, M. G. Savelieff, B. S. Bassil, B. Keita, L. Nadjo, *Inorg. Chem.* **2002**, *41*, 783–789.

[7] K. Nakamoto, *Infrared and Raman Spectra of Inorganic and Coordination Compounds*, Wiley Interscience, New York, USA, **1997**.

[8] C. Rocchiccioli-Deltcheff, M. Fournier, R. Franck, R. Thouvenot, *Inorg. Chem.* **1983**, *22*, 207–216.

[9] a) I. Loose, E. Droste, M. Bösing, H. Pohlmann, M. H. Dickman, C. Rosu, M. T. Pope, B. Krebs, *Inorg. Chem.* **1999**, *38*, 2688–2694; b) B. Krebs, E. Droste, M. Piepenbrink, G. Vollmer, *C. R. Acad. Sci. Ser. IIc* **2000**, *3*, 205–210; c) M. Piepenbrink, E. M. Limanski, B. Krebs, *Z. Anorg. Allg. Chem.* **2002**, *628*, 1187–1191; d) E. M. Limanski, D. Drewes, B. Krebs, *Z. Anorg. Allg. Chem.* **2004**, *630*, 523–528; e) Y. Jeannin, *C. R. Chimie* **2004**, *7*, 1235–1240; f) F. Hussain, M. Reicke, V. Janowski, S. de Silva, J. Futuwi, U. Kortz, *C. R. Chimie* **2005**, *8*, 1045–1056; g) D. Laurencin, R. Villanneau, P. Herson, R. Thouvenot, Y. Jeannin, A. Proust, *Chem. Commun.* **2005**, 5524–5526; h) J.-P. Wang, P.-T. Ma, J. Li, H.-Y. Niu, J.-Y. Niu, *Chem. Asian J.* **2008**, *3*, 822–833; i) Y.-H. Liu, P.-T. Ma, J.-P. Wang, *J. Coord. Chem.* **2008**, *61*, 936–944; j) A. Dolbecq, J.-D. Compain, P. Mialane, J. Marrot, E. Rivière, F. Sécheresse, *Inorg. Chem.* **2008**, *47*, 3371–3378.

[10] U. Kortz, M. G. Savelieff, B. S. Bassil, M. H. Dickman, *Angew. Chem. Int. Ed.* **2001**, *40*, 3384–3386.

[11] I. D. Brown, D. Altermatt, *Acta Crystallogr., Sect. B* **1985**, *41*, 244–247.

[12] C. Tourné, A. Revel, G. Tourné, M. Vendrell, *C. R. Acad. Sci. Paris, Sér. C* **1973**, *277*, 643–645.

[13] *APEX2, version 2.1-0*, Bruker AXS Inc., Madison, Wisconsin, USA, **2005**.

[14] G. M. Sheldrick, *Acta Crystallogr., Sect. A* **2008**, *64*, 112–122.

[15] A. L. Spek, *PLATON*, Utrecht Universiteit, Utrecht, The Netherlands, **2005**.

Received: November 11, 2008
Published Online: January 29, 2009

 © 2009 Wiley-VCH Verlag GmbH & Co. KGaA, Weinheim